Available online at www.sciencedirect.com
ScienceDirect
Journal of Power Sources 169 (2007) 40–46
JOURNAL OF POWER SOURCES
www.elsevier.com/locate/jpowsour

Optimization of glass–ceramic sealant compositions in the system $MgO–BaO–SiO_2$ for solid oxide fuel cells (SOFC)☆

M.J. Pascual[a,*], A. Guillet[b], A. Durán[a]

[a] *Instituto de Cerámica y Vidrio (CSIC), Campus de Cantoblanco, 28049 Madrid, Spain*
[b] *Faculté des Sciences Fondamentales & Appliquées, Université de Poitiers, 86022 Poitiers, France*

Available online 30 January 2007

Abstract

The glass–ceramic with composition 55 SiO_2–27 BaO–18 MgO, mol.% (Mg1.5–55) presents suitable properties for application as a sealant material in IT-SOFC; good unions are achieved with the electrolyte 8YSZ and with the aluminium based interconnect material FeCr alloy. Nevertheless, sealing delaminates when applied to chromium based ferritic stainless steel Crofer 22, one of the most used interconnect material in SOFC, due to the precipitation of $BaCrO_4$ at the interface.

In this work, the union and chemical compatibility of new compositions prepared from modifications of composition Mg1.5–55 have been tested on Crofer 22. The modifications consisted on substituting SiO_2 for B_2O_3 (Mg1.5–50–5B to Mg1.5–35–20B), for B_2O_3 and PbO (Mg1.5–40–5B–10Pb), and B_2O_3 and part of MgO for ZnO (Mg1.5–50–5B–8Zn and Mg1.5–40–15B–8Zn). The characterization of the glass–ceramic materials was carried out by dilatometry, differential thermal analysis (DTA), hot-stage microscopy (HSM), X-ray diffraction (XRD) and scanning electron microscopy (SEM).

All the glasses present a suitable thermal expansion coefficient for use in SOFCs. The addition of B_2O_3 produces the expected decrease of viscosity and a delay in the crystallisation, which gives a better wettability of the glasses on the steel and a better union, inhibiting the direct reaction between chromium oxide and the barium rich crystalline phases to form $BaCrO_4$. At 850 °C, barium silicates crystallize in all the glasses. Barium magnesium silicates and magnesium silicate are present in the glasses without zinc and the crystallisation of barium zinc silicate is promoted in the zinc containing glasses instead. Compositions Mg1.5–40–15B and Mg1.5–40–15B–8Zn exhibit the best glass–ceramic/Crofer 22 union for the operation temperature of 850 °C. The seals are pore-less, strongly adherent to the steel and present elongated crystals which are homogeneously distributed in the glass matrix.

Keywords: Sealing; Glass–ceramic; Interconnect; Crofer 22; SOFC

1. Introduction

A key problem in the fabrication of solid oxide fuel cells of planar configuration and intermediate operation temperature (IT-SOFC) is the sealing of the electrolyte or the ceramic anode with the metallic interconnect in order to achieve a hermetic and stable cell.

The sealing material must provide tightness for avoiding the leakage of reactant gases which implicate that a series of thermal, mechanical and chemical requirements must be fulfilled. Additionally, the sealing must present special characteristics referred to electrical conductivity, fabrication, design and application. The glass–ceramic materials offer the best perspectives to satisfy the requirements [1,2].

In previous works, the composition $55SiO_2{\cdot}27BaO{\cdot}18MgO$ (mol.%) (Mg1.5–55) has been developed as a good candidate for sealing SOFC [3–5]. The bonding with the electrolyte yttria stabilised zirconia (8YSZ) and different types of interconnect materials has been studied, particularly the ferritic stainless steel Crofer 22 and the aluminium based alloy FeCr alloy. The bonding with 8YSZ and FeCr alloy is strong and stable [6].

The oxide layer formed in the surface of the steel FeCr alloy, mainly formed by aluminium oxide, reacts during the sealing with the vitreous matrix originating a strong seal with high stability versus thermal cycling. Nevertheless, the composition does not present bonding with the steel Crofer 22 due to the precipitation of $BaCrO_4$ at the interphase, with a coefficient of thermal expansion (CTE) very different to that of the materials to be joined [7]. By the other hand, in reducing atmosphere, the

☆ This paper is presented at the 2nd National Congress on Fuel Cells, CONAPPICE 2006.

* Corresponding author. Tel.: +34 917355840x1221; fax: +34 917355843.
E-mail address: mpascual@icv.csic.es (M.J. Pascual).

0378-7753/$ – see front matter © 2007 Elsevier B.V. All rights reserved.
doi:10.1016/j.jpowsour.2007.01.040

Table 1
Glass compositions (mol.%)

Glass	SiO_2	BaO	MgO	B_2O_3	PbO	ZnO
Mg1.5–55	55	27	18			
Mg1.5–50–5B	50	27	18	5		
Mg1.5–45–10B	45	27	18	10		
Mg1.5–40–15B	40	27	18	15		
Mg1.5–35–20B	35	27	18	20		
Mg1.5–40–5B–10Pb	40	27	18	5	10	
Mg1.5–50–5B–8Zn	50	27	10	5		8
Mg1.5–40–15B–8Zn	40	27	10	15		8

formation of the chromate phase does not take place, providing strong and stable bonding able to undergo up to 10 cycles of heating and cooling.

Within the ferritic stainless steel, the chromium oxide based alloys (III) seem to be more suitable than the aluminium based alloys to form the interconnect in SOFCs, due to a suitable CTE, low cost and a greater electrical conductivity of Cr_2O_3 compared with that of alumina formed at the steels surface during the cell operation.

In this work, the compatibility of new compositions prepared from modifications of composition Mg1.5–55 has been studied for obtaining good bonding between the cell elements as well as good properties of adherence and tightness. It is expected that the new compositions present a lower tendency to the reaction of chromate formation, due to their lower viscosity, greater wettability on the steel surface and slower crystallisation. A complete thermal characterization of the compositions has been carried out.

2. Experimental procedure

The studied compositions are grouped in Table 1. The ratio BaO/(MgO + ZnO) has been kept constant and equal to 1.5. The raw materials employed for melting the glasses were: silica sand, vitreous boron oxide (Alfa Aesar), barium carbonate (Alfa Aesar), magnesium oxide (Panreac), lead oxide (Aldrich) and zinc oxide (Panreac). The mixtures were calcinated in electrical furnace at 1100 °C and then melted at 1550 °C. The obtained glasses were annealed according to their transition temperature (T_g). The density of the glasses was measured employing the Archimedes method.

Dilatometric measurements of the bulk glasses were carried out employing a differential dilatometer Netzsch Gerätebau model 402 EP.

The glasses were milled in an agate mill with alcohol for 3 h. The glass powder was sieved below 60 μm and the particle size was measured with an equipment Masterizer S, Malver Instruments Ltd. by the method of laser light dispersion.

A hot-stage microscope model EM201 with image analysis and Leica furnace 1750/15 was used for the study of the sintering and fluency kinetics of the original glasses as well as for the determination of viscosity on alumina substrates at a heating rate of 5 °C min^{-1} up to 1300 °C. Measurements were also carried out with the steel Crofer 22 as substrate at a heating rate of 2 °C min^{-1} up to 1000 °C.

DTA measurements were performed with an EXSTAR 6300 (Seiko) instrument using powdered Al_2O_3 as inert reference material and employing 50 ± 5 mg of glass powder in a flowing (50 mL min^{-1}) atmosphere of air; calibration employed In, Zn and Al standards in the same conditions. The heating rate of the experiment was 10 °C min^{-1} in order to obtain narrow and well defined peaks.

The steel Crofer 22 from the company Thyssen Krupp VDM GmbH is one of the most employed materials for interconnects in SOFC [8]. Chromium and manganese oxides are formed on the steel surface at 900 °C. The composition of this steel is in wt.%: Cr (20–20.4), Fe (bal.), C (0.03), Mn (0.3–0.8), Si (0.5), Cu (0.5), P (0.05), Ti (0.03–0.2), La (0.04–0.2).

For the preparation of the bonding (steel/glass/steel), the glass powder was mixed with alcohol to obtain a paste which was spread between two steel plates (1cm length and 0.5 wide). The thermal treatment carried out was: 2 °C min^{-1} up to 850 °C, keeping this temperature during different times, no pressure was applied. Transversal sections of the samples were studied by SEM with a Zeiss microscope model DSM-950 with microprobe for microanalysis by X-ray dispersion energy, EDS TRACOR NORTHEM ZX-II.

Additionally, cylindrical samples of glass powder were isostatically pressed and subjected to the same thermal treatment in an electric furnace. The samples were milled and the corresponding X-ray patterns were obtained with a Siemens diffractometer model D5000.

3. Results and discussion

The density of the glasses, presented in Table 2, situates between 3 and 4 for all the glasses excepting the lead containing one, Mg1.5–40–5B–10Pb. The density increases when increasing the B_2O_3 amount; the only exception appears

Table 2
Density of the glasses and dilatometric results

Glass	d_{glass} (g cm^{-3}) ± 0.05	$\alpha \times 10^6$ K^{-1} ± 0.5	T_g °C ± 3	T_d °C ± 5
Mg1.5–55	3.15	10.1	715	750
Mg1.5–50–5B	3.39	9.7	658	699
Mg1.5–45–10B	3.65	9.9	647	690
Mg1.5–40–15B	3.53	7.9	628	659
Mg1.5–35–20B	3.99	8.6	624	666
Mg1.5–40–5B–10Pb	5.44	12.3	/	512
Mg1.5–50–5B–8Zn	3.03	10.9	/	656
Mg1.5–40–15B–8Zn	3.97	10.5	616	653

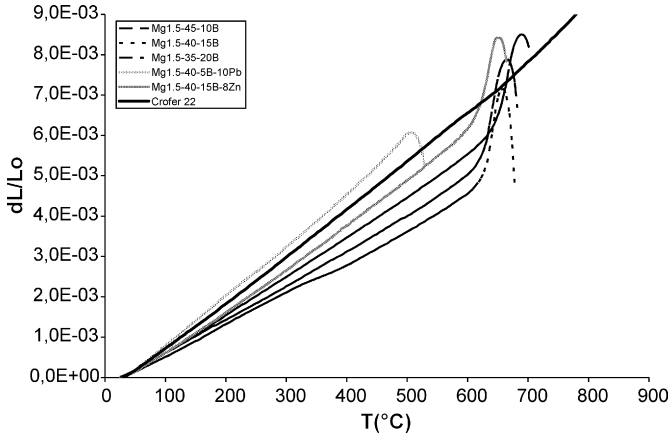

Fig. 1. Dilatometric curve for some studied glasses and the steel Crofer 22.

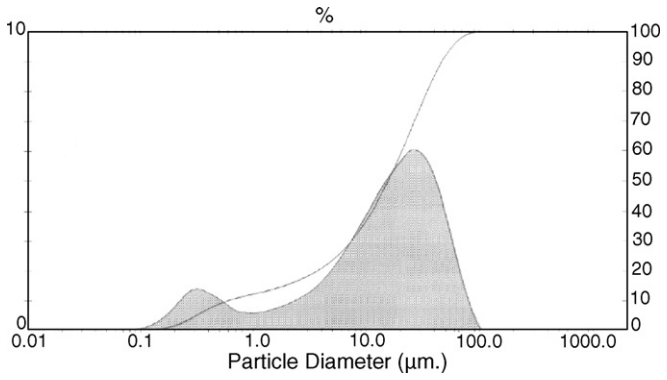

Fig. 2. Particle size distribution of Mg1.5–40–5B–10Pb glass.

for Mg1.5–40–15B, which density is smaller than that of Mg–45–10B, probably due to a change in the B_2O_3 coordination.

Table 2 also presents the dilatometric properties of the glasses and the steel: coefficient of thermal expansion (CTE, α), transition temperature (T_g) and softening temperature (T_d). The CTE decreases when increasing the B_2O_3 content. The lead containing glass Mg1.5–40–5B–10Pb presents a CTE too high along with a T_d low for applications in SOFC. The rest of compositions accomplish the requirements for sealing SOFCs, with CTE between 8–11 $\times 10^{-6}\,K^{-1}$ close to CTE of Crofer 22 ($11.5 \times 10^{-6}\,K^{-1}$). Fig. 1 represents the dilatometric curves of the glasses together with that of the steel Crofer 22.

Fig. 2 shows the particle size distributions for Mg1.5–40–5B–10Pb as an example. The average particle size of the powder for all compositions is around 20 μm.

Fig. 3a–d represents the DTA-TG curves of compositions Mg1.5–40–15B, Mg1.5–35–20B, Mg1.5–40–5B–10Pb and Mg1.5–40–15B–8Zn, carried out at 10 °C min^{-1} up to 1200 °C. The characteristic temperatures of all the glasses (T_g: transformation temperature, T_X: temperature of beginning of crystallisation, T_C: crystallisation temperature) appear in Table 3.

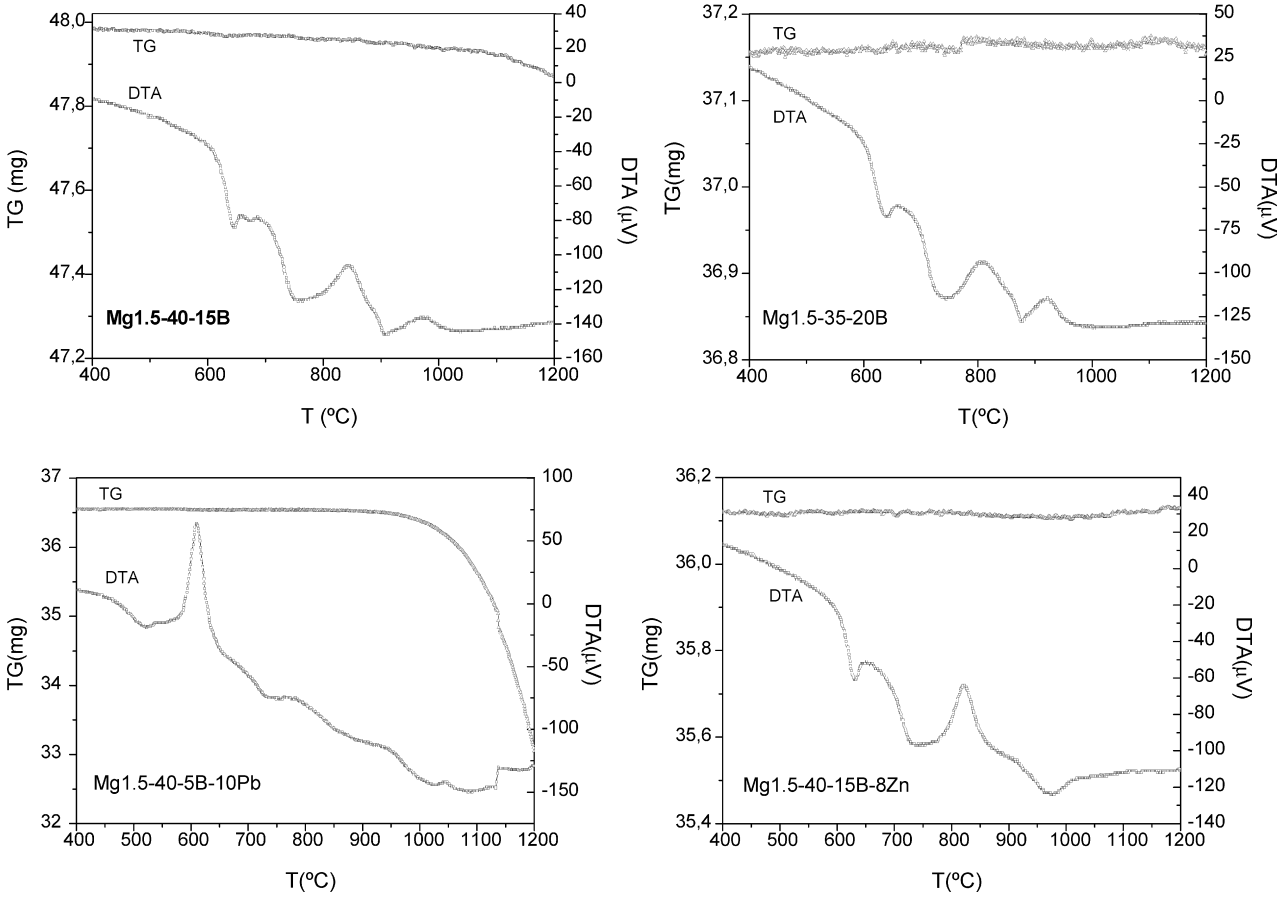

Fig. 3. DTA-TG plots for some studied glasses.

Table 3
DTA results, T (°C)

Glass	T_g (1) ± 7	T_g (2) ± 7	T_X (1) ± 9	T_C (1) ± 9	T_X (2) ± 9	T_C (2) ± 9
Mg1.5–55	699	–	891	918	–	–
Mg1.5–50–5B	670	–	770	800	–	–
Mg1.5–45–10B	660	–	764	814	–	–
Mg1.5–40–15B	640	670	760	845	905	972
Mg1.5–35–20B	630	–	732	805	878	920
Mg1.5–40–5B–10Pb	550	–	615	650	–	–
Mg1.5–50–5B–8Zn	650	–	785	822	–	–
Mg1.5–40–15B–8Zn	620	–	780	820	–	–

Table 4
Characteristic temperatures (°C) obtained by HSM and alumina substrate

Glass	T_{FS} ± 5	T_{MS} ± 5	T_R ± 10	T_{HB} ± 10	T_F ± 5
Mg1.5–55	750	835	1154	1174	1202
Mg1.5–50–5B	700	800	1025	1043	1146
Mg1.5–45–10B	700	790	802	984	1032
Mg1.5–40–15B	700	750	783	899	1052
Mg1.5–35–20B	660	710	760	863	950
Mg1.5–40–5B–10Pb	530	600	920	1021	1094
Mg1.5–50–5B–8Zn	700	790	1020	1036	1078
Mg1.5–40–15B–8Zn	670	735	774	925	1088

Crystallisation temperatures run from 800 to 850 °C, lower than that of initial Mg1.5–55 composition. The glasses with the highest boron content show a second crystallisation peak at higher temperature (920–970 °C). The behaviour of Mg1.5–40–5B–10Pb composition is very different with a very low crystallisation temperature (650 °C) and a significant weight loss from 1000 °C, due to PbO volatilization. These features make this composition not suitable for the sealing application.

HSM tests permitted to determine the temperatures (°C) corresponding to the characteristic viscosity points [9]. First shrinkage (T_{FS}) ($\log \eta = 9.1 \pm 0.1$), maximum shrinkage (T_{MS}) ($\log \eta = 7.8 \pm 0.1$), softening (T_R) ($\log \eta = 6.3 \pm 0.1$), half ball (T_{HB}) ($\log \eta = 4.1 \pm 0.1$) and fluency (T_F) ($\log \eta = 3.4 \pm 0.1$), which are presented in Table 4.

As expected, a progressive decrease of the characteristic temperatures is observed when increasing the B_2O_3 contain (from Mg1.5–55 to Mg1.5–35–20B). If the glasses Mg1.5–40–15B and Mg1.5–40–15B–8Zn, which contain the same boron amount but with part of the MgO substituted for ZnO are compared, the decrease is more pronounced in the latter. From these points, it is possible to plot a viscosity–temperature curve fitted through the Vogel–Fulcher–Tamman (VFT) equation (Fig. 4a and b).

An important decrease of viscosity is observed, particularly for Mg1.5–40–15B, Mg1.5–35–20B and Mg1.5–40–15B–8Zn. Moreover, the viscosity data are not affected by the crystallisation during the HSM measurement. These glasses have a viscosity around $\log \eta = 5$ at 850 °C, suitable to allow a good bonding with the steel but too low to maintain the integrity of the SOFC. Nevertheless, the crystallisation during the elongated thermal treatment at 850 °C allows the necessary increase of viscosity.

The temperatures range around T_R is affected by the crystallisation for glasses Mg1.5–55, Mg1.5–50–5B, Mg1.5–40–5B–10Pb and Mg1.5–50–5B–8Zn. As a consequence, the apparent viscosity obtained through the HSM measurement, is greater than that of the non-crystallised glass at this temperature.

Similarly, HSM was carried out on the steel substrate. In this case, the final temperature of the experiment was 1000 °C, maximum operation temperature of a SOFC. The results appear in Table 5, the existence of bonding or de-bonding is also indicated.

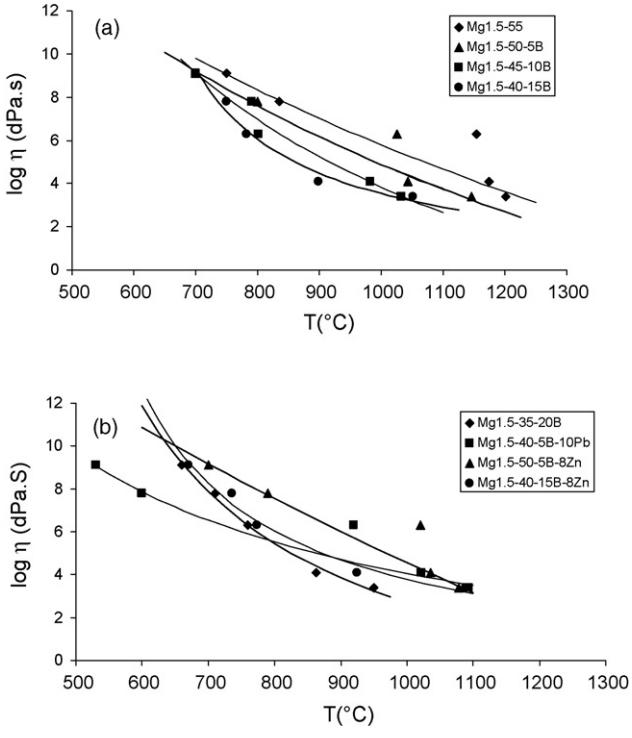

Fig. 4. (a and b) Viscosity–temperature curves for all the studied glasses.

Table 5
Characteristic temperatures (°C) obtained by HSM and steal Crofer22 as substrate

Glass	$T_{FS} \pm 5$	$T_{MS} \pm 5$	$T_R \pm 10$	$T_{HB} \pm 10$	$T_F \pm 5$	Bonding
Mg1.5–55	745	825	/	/	/	No
Mg1.5–50–5B	700	800	/	/	/	No
Mg1.5–45–10B	680	780	800	977	990	Yes
Mg1.5–40–15B	675	747	776	905	932	Yes
Mg1.5–35–20B	650	725	750	867	886	Yes
Mg1.5–40–5B–10Pb	525	580	925	1000	/	Yes
Mg1.5–50–5B–8Zn	700	790	/	/	/	No
Mg1.5–40–15B–8Zn	650	729	767	926	935	Yes

The glasses Mg1.5–55, Mg1.5–50–5B and Mg1.5–50–5B–8Zn do not bond to the steel due to the formation of $BaCrO_4$, their densification curves not presenting the points of softening (R), half ball (HB) and fluency (F). For the other glasses, typical curves of densification and fluency with all the characteristics points (FS, MS, R, HB and F) are obtained all presenting a good bonding with the steel.

The relative initial density of the samples is 0.45–0.55. After shrinkage around 40% when reaching T_{MS} all of them get high densification values around 95%.

The following Table 6 shows the crystalline phases present in the glass–ceramic seals after a thermal treatment of 100 h at 850 °C. Diffractograms for Mg1.5–40–5B–10Pb and Mg1.5–40–15B–8Zn are shown as examples (Fig. 5a and b). The crystalline phases appearing for Mg1.5–55 [10] are barium silicates (B_5S_8 and BS_2) and barium and magnesium silicate (BM_2S_2). Barium silicates crystallize in all the glasses, while barium magnesium silicates and magnesium silicate are present in the glasses without zinc; the crystallisation of barium zinc silicate is promoted in the zinc containing glasses. One single phase, barium magnesium silicate (B_2MS_2) crystallize in Mg1.5–40–5B–10Pb.

The examination of the steel/glass–ceramic seals using optical microscopy indicated that the best bondings are obtained with compositions Mg1.5–40–15B, Mg1.5–35–20B and Mg1.5–40–15B–8Zn. The compositions Mg1.5–45–10B and Mg1.5–50–5B–8Zn showed undesirable porosity.

The SEM micrograph of the union steel/Mg1.5–40–15B–8Zn after 100 h at 850 °C shows that the seal is perfectly adhered to the steel, presenting a homogeneous interphase of around 10 μm (Fig. 6). EDS analysis was carried at the interphase and at different points in the glass–ceramic. It is a semi-quantitative analysis since boron cannot be detected. Point 1 corresponds to the steel composition. Point 2 is located in the interphase, showing the reaction of glass with chromium and manganese, the components of the superficial oxide layer of the steel.

In the glass–ceramic, some diffusion of iron and chromium is observed up to around 50 μm from the joining. The micrograph shows the elongated shape of the crystals present in the glass–ceramic Mg1.5–40–15B–8Zn. The uni-dimensional crystallisation growth mechanism observed in this type of glasses has been previously reported for Mg1.5–55 in [10]. Although no difference is appreciated in secondary electrons among crystals, two different types of crystals are easily differentiated using back-scattered electrons, white crystals (point 5) and smaller dark crystals (point 6). Point 5 analysis corresponds to barium silicate crystals, and point 6 to barium zinc silicate. Zn droplets are observed (point 3), indicating a strong reduction of ZnO which is not explained according to the Ellingham diagrams.

Table 6
Crystalline phases present in the glass–ceramics

Glass	Crystalline phase						
	BS	BS_2	B_2S	MS	BMS	B_2MS_2	BZ_2S_2
Mg1.5–45–10B		√	√	√	√		
Mg1.5–40–15B	√		√	√	√		
Mg1.5–35–20B	√		√	√	√		
Mg1.5–40–5B–10Pb						√	
Mg1.5–50–5B–8Zn	√	√					√
Mg1.5–40–15B–8Zn	√	√					√

B: BaO; S: SiO_2; M: MgO; Z: ZnO.

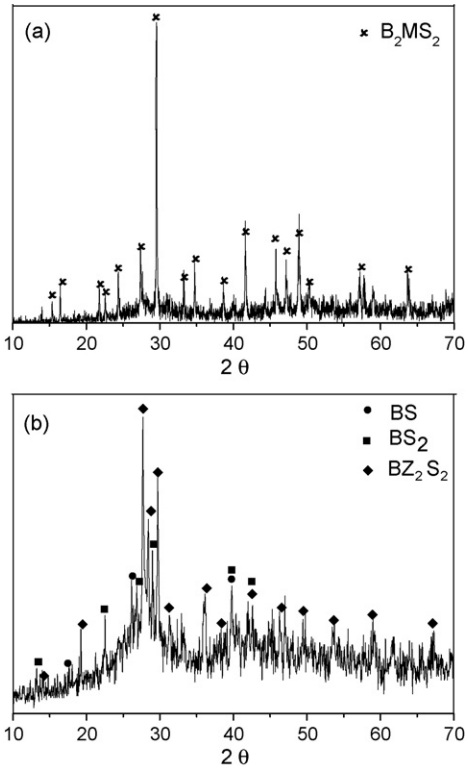

Fig. 5. Diffractograms corresponding to (a) Mg1.5–40–5B–10Pb and (b) Mg1.5–50–5B–8Zn after treatment at 850 °C during 100 h.

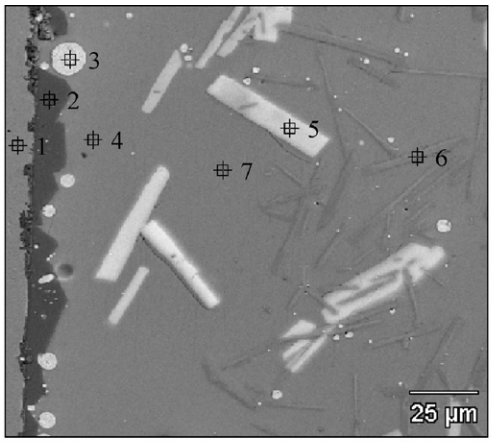

% Weight

	SiO_2	BaO	MgO	ZnO	Fe	Cr	Mn
1	0.26				84.16	12.35	2.77
2	35.58	36.28	0.43	4.64	3.02	19.54	0.52
3		0.69		97.77	1.33	0.20	
4	24.79	63.46	1.49	6.72	1.80	1.74	
5	34.21	65.79					
6	25.17	50.33	4.35	20.14			
7	25.28	65.28	1.46	6.74	0.29	0.79	0.15

Fig. 6. SEM micrographs of the union Crofer 22/Mg1.5–40–15B–8Zn and EDS analysis of some specific points.

Although further work is necessary to explain this behaviour, the presence of metallic Zn could cause problems related to the electrical isolator behaviour of the glass–ceramic.

Fig. 7 shows the SEM micrograph of the joining steel/Mg1.5–40–15B after 100 h at 850 °C. Point 5 shows a compatible and very thin interphase between both materials, enriched in Cr and Mn. The composition of the crystals corresponds to a barium magnesium silicate which is the main phase as obtained by the X-ray diffraction. The adequate viscosity and wettability of this glass allowed getting the seal with the best properties. Different from Mg1.5–55 which is fully crystallized after 100 h at 850 °C [10], this composition results in a partially crystallized material with a relatively large glassy phase volume after the same treatment. Nevertheless, the viscosity is high enough to ensure the

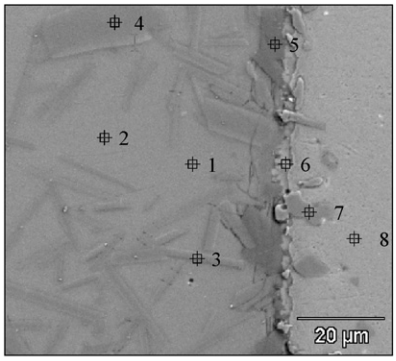

Weight %

	SiO_2	BaO	MgO	Fe	Cr	Mn
1	26.68	67.39	3.36	0.56	1.89	0.13
2	25.44	66.97	3.66	1.43	2.50	
3	30.74	57.26	11.01	0.42	0.67	0.11
4	31.59	54.77	12.88		0.76	
5	43.91	40.14		2.05	13.89	
6	2.24	5.06		31.77	60.03	0.90
7				24.54	75.28	0.18
8				80.71	18.92	0.37

Fig. 7. SEM micrograph of the union Crofer 22/Mg1.5–40–15B and EDS analysis of some specific points.

tightness and mechanical stability of the sealing at the working temperature of the cell. Although the crystallisation temperature of this glass is lower, the kinetics of crystallisation is slower as well, inhibiting the direct reaction of chromium oxide with the barium rich crystalline phases to form $BaCrO_4$.

All exposed results bring to consider the composition Mg1.5–40–15B as the most suitable material for sealing SOFC.

4. Conclusions

The glasses Mg1.5–55, Mg1.5–50–5B, Mg1.5–45–10B, Mg1.5–50–5B–8Zn and Mg1.5–40–15B–8Zn present a suitable thermal expansion coefficient for their use in SOFC ($8–11 \times 10^{-6}\,K^{-1}$). On the other hand, the low crystallisation temperature and the volatilization of lead at the operating temperatures of the cell exclude glass Mg1.5–40–5B–10P to be used in this application.

Barium silicates crystallize in all the glasses, while barium magnesium silicates and magnesium silicate are present in the glasses without zinc; the crystallisation of barium zinc silicate is promoted in the zinc containing glasses.

The addition of B_2O_3 produces an expected decrease of viscosity and delay in the crystallisation which leads to a greater wettability of the glasses on the steel and to a better bonding, which inhibit the formation of $BaCrO_4$. The glasses Mg1.5–40–15B and Mg1.5–40–15B–8Zn produced the best glass–ceramic seals, extent of porosity and presenting crystals of elongated shape homogeneously distributed in the glass matrix and strongly adhered to the steel. These compositions result in partially crystallized materials with a relatively large glassy phase volume. Nevertheless, the viscosity is high enough to ensure the tightness and mechanical stability of the sealing at the working temperature of the cell.

Acknowledgements

The authors thank the CICYT MAT 2003-05902-C02-01 project, the *Ramón y Cajal* programme of the Spanish MEC and to the European *Erasmus* programme.

References

[1] J.W. Fergus, J. Power Sources 147 (2005) 46–57.
[2] C. Lara, M.J. Pascual, A. Durán, Bol. Soc. Esp. Cerám. Vidrio 42 (3) (2003) 133–143.
[3] C. Lara, Glass–ceramic sealants of the system RO–BaO–SiO_2 (R = Zn, Mg) for solid oxide fuel cells (SOFC), PhD Thesis, Autonoma University of Madrid, 2006.
[4] C. Lara, M.J. Pascual, A. Durán, J. Non-Cryst. Solids 348 (2004) 149–155.
[5] C. Lara, M.J. Pascual, R. Keding, A. Durán, J. Power Sources 157 (2006) 377–384.
[6] C. Lara, M.J. Pascual, A. Durán, Phys. Chem. Glasses: Eur. J. Glass Sci. Technol. Part B, (2007), in press.
[7] P. Batfalsky, V.A.C. Haanappel, J. Malzbender, N.H. Menzler, V. Shemet, I.C. Vinke, R.W. Steinbrech, J. Power Sources 155 (2006) 128–137.
[8] www.thyssenkruppvdm.com.
[9] M.J. Pascual, A. Durán, M.O. Prado, Phys. Chem. Glasses 46 (5) (2005) 512–520.
[10] M.J. Pascual, C. Lara, A. Durán, Phys. Chem. Glasses: Eur. J. Glass Sci. Technol. Part B 47 (5) (2006) 572–581.